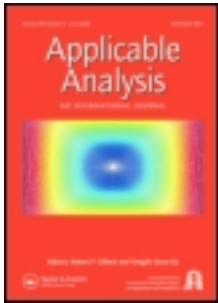


This article was downloaded by: [University of Delaware]

On: 19 June 2013, At: 10:26

Publisher: Taylor & Francis

Informa Ltd Registered in England and Wales Registered Number: 1072954 Registered office: Mortimer House, 37-41 Mortimer Street, London W1T 3JH, UK



Applicable Analysis: An International Journal

Publication details, including instructions for authors and subscription information:

<http://www.tandfonline.com/loi/gapa20>

The inverse scattering problem for a partially coated cavity with interior measurements

Yuqing Hu^a, Fioralba Cakoni^b & Jijun Liu^a

^a Department of Mathematics, Southeast University, 210096, Nanjing, China

^b Department of Mathematical Sciences, University of Delaware, 19716, Newark, Delaware, USA

Published online: 18 Jun 2013.

To cite this article: Yuqing Hu, Fioralba Cakoni & Jijun Liu (2013): The inverse scattering problem for a partially coated cavity with interior measurements, *Applicable Analysis: An International Journal*, DOI:10.1080/00036811.2013.801458

To link to this article: <http://dx.doi.org/10.1080/00036811.2013.801458>

PLEASE SCROLL DOWN FOR ARTICLE

Full terms and conditions of use: <http://www.tandfonline.com/page/terms-and-conditions>

This article may be used for research, teaching, and private study purposes. Any substantial or systematic reproduction, redistribution, reselling, loan, sub-licensing, systematic supply, or distribution in any form to anyone is expressly forbidden.

The publisher does not give any warranty express or implied or make any representation that the contents will be complete or accurate or up to date. The accuracy of any instructions, formulae, and drug doses should be independently verified with primary sources. The publisher shall not be liable for any loss, actions, claims, proceedings, demand, or costs or damages whatsoever or howsoever caused arising directly or indirectly in connection with or arising out of the use of this material.

The inverse scattering problem for a partially coated cavity with interior measurements

Yuqing Hu^a, Fioralba Cakoni^{b*} and Jijun Liu^a

^aDepartment of Mathematics, Southeast University, Nanjing 210096, China; ^bDepartment of Mathematical Sciences, University of Delaware, Newark, Delaware 19716, USA

Communicated by R. Gilbert

(Received 22 January 2013; final version received 29 April 2013)

We consider the interior inverse scattering problem of recovering the shape and the surface impedance of an impenetrable partially coated cavity from a knowledge of measured scatter waves due to point sources located on a closed curve inside the cavity. First, we prove uniqueness of the inverse problem, namely, we show that both the shape of the cavity and the impedance function on the coated part are uniquely determined from exact data. Then, based on the linear sampling method, we propose an inversion scheme for determining both the shape and the boundary impedance. Finally, we present some numerical examples showing the validity of our method.

Keywords: inverse scattering; mixed boundary value problem; boundary impedance; interior measurements; linear sampling method

AMS Subject Classifications: 35R30; 65F22; 65R20; 65R32

1. Introduction

The inverse scattering problem for acoustic or electromagnetic waves has drawn increased attention in recent years due to its importance in various applications. In the past 10 years, considerable progress is made in the development of the so-called qualitative methods (otherwise known as non-iterative methods) for solving the inverse scattering problem, [1–4] as an alternative approach to optimization techniques.[5] Typically in applications such as radar, sonar, medical imaging, underground imaging, transmitters and receivers are situated outside the target, and then different inversion techniques can be used to extract information on the target from these external measurements [6–11,32,33] (and references therein). However, in non-destructive testing of the integrity of the interior of devices, one needs to solve the inverse problem with interior measurements obtained from receivers and transmitters located inside the device. Thus, in the case of a impenetrable cavity, the forward scattering problem is formulated as an interior boundary value for the scattered field. Recently, the inverse problem for cavities with interior measurements has been considered in many papers. More specifically, in [12,13] the authors use the linear sampling method to determine the shape of a cavity with Dirichlet and impedance boundary condition for the scalar Helmholtz equation, whereas in [14] the authors generalize these ideas to Maxwell's

*Corresponding author. Email: cakoni@math.udel.edu

equation. In [15], the inverse interior scattering problem for a cavity with Dirichlet boundary conditions is considered, and a Newton-type optimization technique for an equivalent non-linear integral equation is employed to solve the problem. Other methods have been applied in [16–18] to solve the interior inverse problem of shape reconstruction. All the aforementioned work is limited to reconstructing only the shape of the cavity. In this work, we revisit the inverse acoustic or electromagnetic scattering problem for an impenetrable cavity with internal measurements. We assume that (e.g. in the context of electromagnetic scattering) part of cavity’s wall is made of perfectly conducting material and the other part is coated by a thin layer of absorbing material. The forward problem corresponding to the scattering of an interior point source by this cavity becomes an interior mixed boundary value problem with Dirichlet–Robin boundary condition. Our goal is to determine the shape and the impedance function from a knowledge of scattered fields measured on a curve inside the cavity due to point sources located on the same curve. We use the near field linear sampling method to determine the shape of the cavity (see [6] for the case of exterior inverse scattering problem) and then following [7,8] based on the solution of the near field equation used for the linear sampling method, we derive an integral equation to determine the impedance function. We mention that other type of qualitative methods have also been used for the case of exterior scattering problems to determine boundary physical properties in addition to the shape.[10,19]

Our paper is organized as follows. In the next section, we formulate the direct and inverse scattering problem and prove a uniqueness result for the inverse problem. In addition, we discuss an exterior mixed boundary value problem which is an auxiliary essential tool for our reconstruction technique. Due to the “wrong” sign of the impedance, this exterior problem could give rise to eigenfrequencies for which our inversion method fails. However, we prove that this bad frequencies form at most a discrete set. In Section 3, we proceed with mathematical development of the inversion algorithm for reconstructing the shape as well the boundary impedance of the cavity. The reconstruction of the shape is based on a linear sampling method for which we solve a linear ill-posed integral equation on a closed (measurements) curve. Then the solution of this equation is used in an other integral equation to determine the surface impedance function. We end the paper with various numerical examples of reconstruction for the shape and impedance function.

2. The inverse cavity problem with mixed boundary conditions

Let $D \subset \mathbb{R}^2$ be a bounded connected region with Lipschitz boundary ∂D which is split as $\partial D = \overline{\partial D_D} \cup \overline{\partial D_I}$, where ∂D_D and ∂D_I are disjoint, relatively open subsets of ∂D . Denote by ν the unit outward normal to ∂D defined almost everywhere. We assume that ∂D is the boundary of the cross-section of a cylindrical partially coated perfectly conducting cavity where ∂D_I represents the portion coated by a conducting material. Let $\lambda \in L_\infty(\partial D_I)$ such that $\lambda(x) > 0$ for $x \in \partial D_I$, denote the surface impedance function. For a particular polarization of incident waves, the scattering of electromagnetic waves by this cylindrical cavity at a fixed frequency is modelled by a two-dimensional Helmholtz equation (for simplicity of our presentation, here we consider the two-dimensional case: our analysis is also valid in the three-dimensional case). More specifically, the scattered wave $u^s := u^s(\cdot, z)$ inside D due to an incident point source located at $z \in D$ given by

$$\Phi(\cdot, z) = \frac{i}{4} H_0^{(1)}(k|\cdot - z|)$$

where $H_0^{(1)}$ is the Hankel function of the first kind of order zero, is a solution to

$$\Delta u^s + k^2 u^s = 0, \quad x \in D,$$

such that the total wave $u = u^s(\cdot, z) + \Phi(\cdot, z)$ satisfies the boundary condition

$$\begin{cases} u = 0 & x \in \partial D_D, \\ \frac{\partial u}{\partial \nu} - ik\lambda(x)u = 0 & x \in \partial D_I. \end{cases} \quad (1)$$

Thus, the forward problem in terms of the scattered wave becomes the following interior mixed boundary value problem

$$\begin{cases} \Delta u^s + k^2 u^s = 0 & x \in D, \\ u^s = -\Phi(\cdot, z) & x \in \partial D_D, \\ \frac{\partial u^s}{\partial \nu} - ik\lambda(x)u^s = -\frac{\partial \Phi(\cdot, z)}{\partial \nu} + ik\lambda(x)\Phi(\cdot, z) & x \in \partial D_I. \end{cases} \quad (2)$$

In order to formulate the scattering problem more precisely we need to recall the definition of the following Sobolev spaces.[20] To this end let $\Gamma_0 \subseteq \Gamma$ be an open subset of ∂D . If $H^1(D)$, $H_{loc}^1(\mathbb{R}^2 \setminus \bar{D})$ denote the usual Sobolev spaces and $H^{1/2}(\Gamma)$ their usual trace space, we define:

$$\begin{aligned} H^{\pm 1/2}(\Gamma_0) &:= \{u|_{\Gamma_0} : u \in H^{\pm 1/2}(\Gamma)\} \\ \tilde{H}^{\pm 1/2}(\Gamma_0) &:= \{u \in H^{\pm 1/2}(\Gamma) : \text{supp } u \subseteq \bar{\Gamma}_0\} \\ H^{-1/2}(\Gamma_0) &:= \left(\tilde{H}^{1/2}(\Gamma_0)\right)' \text{ the dual space of } \tilde{H}^{1/2}(\Gamma_0) \\ \tilde{H}^{-1/2}(\Gamma_0) &:= \left(H^{1/2}(\Gamma_0)\right)' \text{ the dual space of } H^{1/2}(\Gamma_0) \end{aligned}$$

The scattering problem (2) is a particular case of the following interior mixed boundary value problem for the Helmholtz equation:

$$\begin{cases} \Delta v + k^2 v = 0 & x \in D, \\ v = f & x \in \partial D_D, \\ \frac{\partial v}{\partial \nu} - ik\lambda(x)v = h & x \in \partial D_I, \end{cases} \quad (3)$$

where $f \in H^{\frac{1}{2}}(\partial D_D)$, $h \in H^{-\frac{1}{2}}(\partial D_I)$. Based on an integral equation method [6,20] or a variational approach,[1] it can be shown that the above scattering problem has a unique solution $u^s \in H^1(D)$ which depends continuously on the boundary data, i.e.

$$\|u\|_{H^1(D)} \leq C \left(\|f\|_{H^{\frac{1}{2}}(\partial D_D)} + \|h\|_{H^{-\frac{1}{2}}(\partial D_I)} \right). \quad (4)$$

The *inverse scattering problem* is: given scattered waves $u^s(\cdot, z)$ on some smooth closed curve C inside D for all source locations $z \in C$, determine the shape ∂D and the impedance function $\lambda(x)$ on ∂D_I (∂D_D could possibly be empty set).

2.1. Uniqueness of the inverse problem

In this section, we show that our multi-static data defined above, uniquely determine ∂D , $\lambda(x)$ and of course its support ∂D_I . Let C be a smooth closed curve and let us define the admissible set of cavities

$$\mathbb{S} := \{D \subset \mathbb{R}^2 : \partial D \text{ is Lipschitz and } D \text{ contains } C \text{ in its interior.}\}$$

Throughout the paper, we assume that k^2 is not a Dirichlet eigenvalue for $-\Delta$ in the interior of C . Note that this is not a restriction since we can easily choose a measurement curve C that satisfies this assumption.

THEOREM 2.1 *Assume that $D_1, D_2 \in \mathbb{S}$ are two cavities having mixed Dirichlet–Robin boundary conditions with surface impedance functions λ_1 and λ_2 , respectively, such that the corresponding scattered fields coincide on C for all point sources located in C and a fixed wave number. Then $D_1 = D_2$, $\partial D_{1,I} = \partial D_{2,I}$ and $\lambda_1(x) = \lambda_2(x)$.*

Proof We denote by G the connected component of $D_1 \cap D_2$ which contains the region bounded by C . Let $u_j^s(\cdot, z)$ be the solution of (2) corresponding to $D_j, \lambda_j, j = 1, 2$. We have that $u_1^s(x, z) = u_2^s(x, z)$ for $x, z \in C$. Following the argument in [12], the latter implies that $u_1^s(x, z) = u_2^s(x, z)$ for $x, z \in \overline{G}$.

Step 1 Uniqueness of D . First we prove $\partial D_1 = \partial D_2$, using the standard argument by Kirsch and Kress in [5] Theorem 5.6 which we sketch here for sake of reader's convenience. To this end, assume that $D_1 \neq D_2$. Then, without loss of generality, we can choose $x^* \in \partial G$ and $x^* \in \partial D_1$, but $x^* \notin \partial D_2$ such that either $\Omega_\epsilon(x^*) \cap \partial D_1 \subset \partial D_{1D}$ or $\Omega_\epsilon(x^*) \cap \partial D_1 \subset \partial D_{1I}$, where $\Omega_\epsilon(x^*)$ is a small disk centred at x^* with radius ϵ . We denote by B_1 the boundary condition on $\partial D_1 \cap \Omega_\epsilon$ which can be either Dirichlet or Robin. Choose $h > 0$ small enough such that

$$z_n := x^* + \frac{h}{n} \nu(x^*) \in G, \quad n = 1, 2, \dots,$$

where ν is the unit normal vector to the boundary ∂D_1 directed into the interior of D_1 . Next, we consider the solutions $u_{n,j}^s(x)$ to the scattering problem (2) corresponding to $D = D_j$ and $\lambda = \lambda_j$ for $j = 1, 2$ on the coated part, with z replaced by z_n , that is, $u_{n,j}^s(x) := u_j^s(x, z_n)$. Hence $u_{n,1}^s(x) = u_{n,2}^s(x)$ for $x \in \overline{G}$ and all $x_n \in G$. Then by (4) on one hand we have that

$$\begin{aligned} \lim_{n \rightarrow \infty} \|B_1 u_1^s(x, z_n)\|_{H^s(\partial G \cap \Omega_\epsilon)} &= \lim_{n \rightarrow \infty} \|B_1 u_2^s(x, z_n)\|_{H^s(\partial G \cap \Omega_\epsilon)} \\ &= \|B_1 u_2^s(x, x^*)\|_{H^s(\partial G \cap \Omega_\epsilon)}, \end{aligned}$$

and on the other hand

$$\lim_{n \rightarrow \infty} \|B_1 u_1^s(x, z_n)\|_{H^s(\partial G \cap \Omega_\epsilon)} = \lim_{n \rightarrow \infty} \|B_1 \Phi(x, z_n)\|_{H^s(\partial G \cap \Omega_\epsilon)} = \infty,$$

where $s = 1/2$ if B_1 is Dirichlet boundary operator or $s = -1/2$ if B_1 is Robin boundary operator. This contradiction proves that $D_1 = D_2$.

Step 2 Uniqueness of λ and ∂D_I . Next we show that the support of the impedance function and the impedance function are uniquely determined. We can prove the uniqueness of ∂D_I from a knowledge of the scattered field in C corresponding to one point source located at $z_0 \in C$. To this end let us show that $\partial D_{1D} = \partial D_{2D}$ and consequently $\partial D_{1I} = \partial D_{2I}$. If $\partial D_{2D} \subset \partial D_{1D}$ is not true then let $\Gamma \subset \partial D_{2D} \setminus (\partial D_{2D} \cap \partial D_{1D}) \neq \emptyset$ be a connected boundary arc. Note that from [12] we have already that the total fields $u := u_1(x, z_0) = u_2(x, z_0)$ coincide in $D := D_1 = D_2$ (note that total field $u_j(x, z_0) = u_j^s(x, z_0) + \Phi(x, z_0)$ where j correspond to D with ∂D_j and $\lambda_j, j = 1, 2$), whence from the Dirichlet boundary condition for $D_2, u = 0$ on Γ in the sense of the trace. Since $\Gamma \subset \partial D_{1I}$, then from the

impedance boundary condition for D_1 we have that $\frac{\partial u}{\partial \nu} - ik\lambda_1 u = 0$ on Γ , hence $\frac{\partial u}{\partial \nu} = 0$ on Γ . Using Holmgren's theorem we know $u(x) = 0$ for all $x \in D \setminus \{z_0\}$, noticing that the total wave $u(x)$ is analytic everywhere in D except the interior point z_0 . Therefore, we have $u^s(x, z_0) = -\Phi(x, z_0)$, $x \neq z_0$ which means that the scattered field blows up as $x \rightarrow z_0$ is a contradiction. Thus, $\partial D_{2D} \subset \partial D_{1D}$. Similarly we can prove $\partial D_{1D} \subset \partial D_{2D}$, which proves the uniqueness of ∂D_I .

Finally, we establish that $\lambda_1 = \lambda_2$ on ∂D_I . If ∂D_I is smooth and λ is continuous we show that one point source is sufficient to uniquely determine λ . Indeed, let as in the above $u_1 := u_1(x, z_0)$ and $u_2 := u_2(x, z_0)$ be the total fields corresponding to λ_1 and λ_2 , respectively, and recall that $u := u_1 = u_2$ in D . In particular

$$u_1 = u_2, \quad \frac{\partial u_1}{\partial \nu} = \frac{\partial u_2}{\partial \nu} \quad \text{on } \partial D_I.$$

Subtracting the boundary condition for u_2 from the boundary condition for u_1 on ∂D_I we have

$$(\lambda_1 - \lambda_2)u = 0 \quad \text{on } \partial D_I \tag{5}$$

Suppose that $\lambda_1 \neq \lambda_2$ at some point $x^* \in \partial D_I$, then it follows from continuity of $\lambda_j(x)$ that there exists a neighbourhood of x^* such that $\lambda_1(x) - \lambda_2(x) \neq 0$ in $O(x^*, \varepsilon) \cap \partial D_I$, which implies $u = 0$ and from the impedance boundary condition $\frac{\partial u}{\partial \nu} = 0$ on $O(x^*, \varepsilon) \cap \partial D_I$. Then the contradiction is obtained in the same way as in the proof of uniqueness of ∂D_I .

For $\lambda \in L_\infty(\partial D_I)$ and ∂D Lipschitz, in Section 3.2 we provide an alternative proof for the uniqueness of λ using the full set of data, i.e. from a knowledge of the scattered fields $u^s(x, z)$ for all $x, z \in C$. □

Having proven the uniqueness, the rest of the paper is devoted to deriving reconstruction algorithms for both ∂D and λ . We end this section by analysing the following exterior mixed boundary value problem corresponding to (3) which will be needed in our later analysis: given $f \in H^{\frac{1}{2}}(\partial D_D)$ and $h \in H^{-\frac{1}{2}}(\partial D_I)$, find $w \in H_{loc}^1(\mathbb{R}^2 \setminus \bar{D})$ such that

$$\begin{cases} \Delta w + k^2 w = 0 & \text{in } \mathbb{R}^2 \setminus \bar{D}, \\ w = f & \text{on } \partial D_D, \\ \frac{\partial w}{\partial \nu} - ik\lambda(x)w = g & \text{on } \partial D_I, \\ \lim_{r \rightarrow \infty} \sqrt{r} \left(\frac{\partial w}{\partial r} - ikw \right) = 0, \end{cases} \tag{6}$$

where $\lambda \in L^\infty(\partial D_I)$, $\lambda(x) > 0$. Due to the opposite sign of the impedance which is not compatible to the decaying condition of outgoing waves,[5] this exterior problem may have real eigenvalues, i.e the uniqueness may fail for a discrete (possibly empty) set of values of $k > 0$, which we refer to as exterior eigenvalues. To study (6), we use a variational approach by first re-writing it as an equivalent problem in a bounded domain. Let Ω be a large disk containing D , $\tilde{f} \in H^{\frac{1}{2}}(\partial D)$ be a bounded extension of f , and $w_0 \in H^1(\Omega \setminus \bar{D})$ be such that $w_0 = \tilde{f}$ on ∂D and w_0 supported in a small neighbourhood of ∂D . Then (6)

is equivalent to finding $v \in H^1(\Omega \setminus \bar{D})$ such that

$$\begin{cases} \Delta v + k^2 v = -\Delta w_0 - k^2 w_0 & \text{in } \Omega \setminus \bar{D}, \\ v = 0 & \text{on } \partial D_D, \\ \frac{\partial v}{\partial \bar{v}} - ik\lambda(x)v = \tilde{h} & \text{on } \partial D_I, \\ \frac{\partial v}{\partial v} = T_k v & \text{on } \partial \Omega, \end{cases} \quad (7)$$

where, $v = w - w_0$, $T_k : H^{\frac{1}{2}}(\partial\Omega) \rightarrow H^{-\frac{1}{2}}(\partial\Omega)$ is the exterior Dirichlet to Neumann operator (see [1] Definition 5.8), and $\tilde{h} := h - \frac{\partial w_0}{\partial v} + ik\lambda(x)w_0$ (see [1], Theorem 8.5). Defining

$$X := \{u \in H^1(\Omega \setminus \bar{D}) : u|_{\partial D_D} = 0\}$$

(7) can be written in the following variational form: find $v \in X$ such that

$$b_k(v, \varphi) + c_k(w, \varphi) = F(\varphi) \quad \text{for all } \varphi \in X, \quad (8)$$

where the sesquilinear forms $b_k(\cdot, \cdot)$ and $c_k(\cdot, \cdot)$ on $X \times X$ are given by

$$\begin{aligned} b_k(v, \varphi) &= \int_{\Omega \setminus \bar{D}} \nabla v \nabla \bar{\varphi} dx - \int_{\partial\Omega} T_0 v \bar{\varphi} ds + ik \int_{\partial D_I} \lambda v \bar{\varphi} ds, \quad v, \varphi \in X, \\ c_k(v, \varphi) &= - \int_{\Omega \setminus \bar{D}} k^2 v \bar{\varphi} dx - \int_{\partial\Omega} (T_k - T_0) v \bar{\varphi} ds, \quad v, \varphi \in X, \end{aligned}$$

where the operator T_0 is given as in [1] Theorem 5.20, and the bounded conjugate linear functional F on X is defined by

$$F(\varphi) := \int_{\Omega \setminus \bar{D}} (\Delta v + k^2 v) \bar{\varphi} dx - \int_{\partial D_I} \tilde{h} \bar{\varphi} ds.$$

From Theorem 5.20 in [1] and Poincaré's inequality in X (assuming that $\partial D_D \neq \emptyset$; if the latter is not true one can use the coercivity of $-T_0$) we obtain

$$\operatorname{Re} b_k(v, \bar{v}) = \int_{\Omega \setminus \bar{D}} |\nabla v|^2 dx + \int_{\partial\Omega} -T_0 v \bar{v} ds \geq C \|v\|_{H^1(\Omega \setminus \bar{D})}^2$$

which by means of Riesz representation theorem gives rise to an invertible operator $B_k : X \rightarrow X$ defined by $b_k(w, \varphi) = (B_k w, \varphi)_X$. Furthermore, due to compactly embedding of $H^1(\Omega \setminus \bar{D})$ into $L^2(\Omega \setminus \bar{D})$ and the fact that $T_k - T_0 : H^{\frac{1}{2}}(\partial\Omega) \rightarrow H^{-\frac{1}{2}}(\partial\Omega)$ is compact (Theorem 5.20 in [1]), we have that $C_k : X \rightarrow X$ defined by $c_k(w, \varphi) = (C_k w, \varphi)_X$ is compact. Hence, the solvability of the exterior impedance problem (6) is equivalent to the invertibility of the operator

$$B_k + C_k \text{ or } I + B_k^{-1} C_k.$$

Let us denote by W_k the compact operator $W_k := B_k^{-1} C_k$.

THEOREM 2.2 *The exterior mixed boundary problem (6) has a unique solution for all values of $k > 0$ except for a discrete (possibly empty) set with $+\infty$ as the only accumulation point. This solution (if it exists) depends continuously on the boundary data.*

Proof From the above, we need to investigate the invertibility of $I + W_k$. Since W_k is compact, we have that the uniqueness implies that the inverse of $I + W_k$ exists and is bounded. To prove that the uniqueness fails for at most a discrete set of values of k we use

the analytic Fredholm theory.[5] Consider a strip \mathcal{D} in the complex plane \mathbb{C} around positive real axis and $I + W_k : \mathcal{D} \rightarrow \mathcal{L}(X)$. The operator B_k and C_k are analytic on k in \mathcal{D} , which implies that W_k is also analytic. Note that the Dirichlet to Neumann operator T_k depends analytically on $k \in \mathbb{C}$ such that $\text{Re}(k) > 0$ (since we are in \mathbb{R}^2 we are excluding $k = 0$ due to the particular behavior of the solution at infinity, however T_k is still continuous at $k = 0$ in the operator norm see Theorem 5.20 in [1]). Obviously, $B_0 + C_0$ is invertible and by continuity it is invertible for some $k_0 > 0$ sufficiently small, whence $I + W_{k_0}$ is invertible. Hence, an application of Theorem 8.26 in [5] proves our claim. \square

Definition 2.3 The values of $k > 0$ for which the homogeneous exterior mixed boundary value problem (6) has a non-trivial solution are called exterior eigenvalues.

3. The solution of the inverse problem

First, we remind the reader that the assumption that k^2 is not a Dirichlet eigenvalue for $-\Delta$ in the region bounded by the measurements curve C holds throughout the paper. Our data-set, i.e. the scattered fields $u^s(x, y)$ for $x \in C$ corresponding to all point sources for $y \in C$ defines the data operator $M : L^2(C) \rightarrow L^2(C)$ by

$$(Mg)(x) = \int_C u^s(x, y)g(y)ds(y) \quad g \in L^2(C), \quad x \in C \tag{9}$$

which is obviously compact as an integral operator with analytic kernel. The following linear integral equation

$$(Mg)(x) = \Phi(x, z) \quad x \in C, \tag{10}$$

will play an important role in our inversion algorithm and will be refer to as the data equation. To understand the data operator, we define the linear operator $B : H^{\frac{1}{2}}(\partial D_D) \times H^{-\frac{1}{2}}(\partial D_I) \rightarrow L^2(C)$ mapping the boundary value (f, h) to the solution v of the corresponding interior mixed boundary value problem (3) evaluated on C . In addition, we define the linear operator $H : L^2(C) \rightarrow H^{\frac{1}{2}}(\partial D_D) \times H^{-\frac{1}{2}}(\partial D_I)$

$$(Hg)(x) = \begin{cases} \omega_g(x) & x \in \partial D_D, \\ \frac{\partial \omega_g}{\partial \nu}(x) - ik\lambda(x)\omega_g(x) & x \in \partial D_I, \end{cases} \tag{11}$$

where ω_g is the single layer potential

$$\omega_g(x) := \int_C \Phi(x, y)g(y)ds(y), \quad x \in \mathbb{R}^2 \setminus C. \tag{12}$$

By linearity and superposition $M = -BH$ and hence the data equation (10) can be written as

$$-(BHg) = \Phi(x, z).$$

LEMMA 3.1 *If k is not an exterior eigenvalue then the data operator M defined by (9) is injective and has dense range.*

Proof If $Mg = 0$ then the scattered field corresponding to ω_g as incident wave is zero on C . By the uniqueness of the Dirichlet problem inside C it is zero inside C and hence from analytic continuation it is zero everywhere in D (note that the scattered field is a solution of the Helmholtz equation in D and thus is analytic in D). But since ω_g satisfies the same mixed boundary conditions on ∂D as the negative scattered field, by the trace theorem we have that $\omega_g = 0$ on ∂D_D and $\frac{\partial \omega_g}{\partial \nu} - ik\lambda(x)\omega_g = 0$ on ∂D_I . The latter implies that ω_g satisfies the homogeneous exterior mixed boundary value problem (6) and hence from the assumptions on k , $\omega_g = 0$ in $\mathbb{R}^2 \setminus C$ (outside C because the uniqueness of (6) and analytic continuation, and inside C from the uniqueness of the Dirichlet problem). The jump condition for the normal derivative of the single layer potential ω_g across C implies that $g = 0$ which proves the injectivity of M . Next, it is easily seen that the L^2 -adjoint M^* of M is given by $M^*h = \overline{Mh}$, whence the adjoint operator M^* is also injective, which implies that M has dense range. \square

LEMMA 3.2 *Assume that k is not an exterior eigenvalue. The bounded linear operator $B : H^{\frac{1}{2}}(\partial D_D) \times H^{-\frac{1}{2}}(\partial D_I) \rightarrow L^2(C)$ is compact, injective and has dense range.*

Proof We choose a disk Ω_r of radius $r > 0$ such that $C \subset \Omega_r \subset D$. Then we can decompose the operator B as $B = B_1 B_2$ where $B_2 : H^{\frac{1}{2}}(\partial D_D) \times H^{-\frac{1}{2}}(\partial D_I) \rightarrow H^{-\frac{1}{2}}(\partial \Omega_r) \times H^{\frac{1}{2}}(\partial \Omega_r)$ is defined by

$$B_2(f, h)(x) = \left(\frac{\partial u^s}{\partial \nu} |_{\partial \Omega_r}, u^s |_{\partial \Omega_r} \right),$$

and $B_1 : H^{-\frac{1}{2}}(\partial \Omega_r) \times H^{\frac{1}{2}}(\partial \Omega_r) \rightarrow L^2(C)$ is defined by

$$B_1(f, h)(x) = \int_{\partial \Omega_r} \left\{ f(y)\Phi(x, y) - h(y) \frac{\partial \Phi(x, y)}{\partial \nu(y)} \right\} ds(y), \quad x \in C,$$

where we use the Green's representation formula of the solution v in Ω_r . [5] Clearly, the operator B_2 is bounded, and B_1 is compact as an integral operator with analytic kernel, [21] which implies that B is compact.

To show that B is injective, let $B(f, h) = 0$. Hence by the definition of B we have that the corresponding solution v of boundary value problem (3) is zero on C (note that v satisfies the Helmholtz equation $\Delta v + k^2 v = 0$ in D and hence is analytic inside D . [1]) Since k^2 is not a Dirichlet eigenvalue in the interior of the curve C , then by the uniqueness of the Dirichlet boundary value problem for Helmholtz equation inside C , we obtain $v = 0$ in the interior of C . Thus by analyticity of v in D we obtain that $v = 0$ in D whence from the trace theorem $f = 0$ and $h = 0$. Finally, since the range of B contains the range of M , we conclude from Lemma 3.1 that the range of B is dense. \square

The following lemma plays an important role for the linear sampling method.

LEMMA 3.3 *The fundamental solution $\Phi(x, z) = \frac{i}{4} H_0^{(1)}(k|x - z|)$ for $x \in C$, is in the range of B if and only if $z \in \mathbb{R}^2 \setminus D$.*

Proof The proof proceeds exactly in the same way as the proof of Theorem 4.2 in [12]. \square

Finally, we need the following approximation result.

LEMMA 3.4 *Assume that k is not an exterior eigenvalue. The range of the operator $H : L^2(C) \rightarrow H^{\frac{1}{2}}(\partial D_D) \times H^{-\frac{1}{2}}(\partial D_I)$ defined by (11) is dense. In other words, any pair $(f, h) \in H^{\frac{1}{2}}(\partial D_D) \times H^{-\frac{1}{2}}(\partial D_I)$ can be approximated arbitrarily close by an Hg in $H^{\frac{1}{2}}(\partial D_D) \times H^{-\frac{1}{2}}(\partial D_I)$.*

Proof Let us define the dual operator $H^\top : \tilde{H}^{-\frac{1}{2}}(\partial D_D) \times \tilde{H}^{\frac{1}{2}}(\partial D_I) \rightarrow L^2(C)$ such that $\langle Hg, (\phi, \psi) \rangle = \langle g, H^\top(\phi, \psi) \rangle$ in the duality pairing sense. By changing the order of integration, it is easy to see that

$$H^\top(\phi, \psi) := \int_{\partial D_D} \Phi(x, y)\phi(y)ds(y) + \int_{\partial D_I} \left(\frac{\partial \Phi(x, y)}{\partial \nu} - ik\lambda\Phi(x, y) \right) \psi(y)ds(y),$$

for $x \in C$. It suffices to show that H^\top is injective since

$$\overline{(\text{Range } H)} = {}^a\text{Kernel } H^\top$$

where a denotes the annihilator (see [20] page 23). To this end let us assume that $H^\top(\phi, \psi) = 0$. We define the potential

$$\mathcal{P}(x) := \int_{\partial D_D} \Phi(x, y)\phi(y)ds(y) + \int_{\partial D_I} \left(\frac{\partial \Phi(x, y)}{\partial \nu} - ik\lambda\Phi(x, y) \right) \psi(y)ds(y),$$

$x \in \mathbb{R}^2 \setminus \partial D$. Since ϕ and ψ have zero extensions in $H^{-\frac{1}{2}}(\partial D)$ and $H^{\frac{1}{2}}(\partial D)$, respectively, [1] \mathcal{P} is well defined in $H_{loc}^1(\mathbb{R}^2 \setminus \partial D)$ and satisfies the Helmholtz equation in D and in $\mathbb{R}^2 \setminus \bar{D}$ (see [20] for the mapping properties of the boundary integral operators in Sobolev spaces). From the assumption we have that $\mathcal{P}(x) = 0$ on C and from the uniqueness of the Dirichlet problem $\mathcal{P}(x) = 0$ inside C also. Since \mathcal{P} satisfies the Helmholtz equation in D , we obtain by unique continuation that $\mathcal{P}(x) = 0$ in D . Thus approaching the boundary ∂D from the inside, we obtain by the trace theorem that $\mathcal{P}^- = 0$ and $\frac{\partial \mathcal{P}^-}{\partial \nu} = 0$ on ∂D . The jump relations across ∂D of single and double layer potential imply

$$\begin{aligned} \mathcal{P}^+ - \mathcal{P}^- &= 0 & \text{on } \partial D_D, & \quad \mathcal{P}^+ - \mathcal{P}^- = \psi & \text{on } \partial D_I \\ \frac{\partial \mathcal{P}^+}{\partial \nu} - \frac{\partial \mathcal{P}^-}{\partial \nu} &= -\phi & \text{on } \partial D_D, & \quad \frac{\partial \mathcal{P}^+}{\partial \nu} - \frac{\partial \mathcal{P}^-}{\partial \nu} = ik\lambda\psi & \text{on } \partial D_I \end{aligned}$$

where $+$ and $-$ indicate that we approach the boundary ∂D from outside and inside, respectively (recall that ν is oriented outside to D). Hence, we have that \mathcal{P} is a radiating solution of the Helmholtz equation and satisfies the boundary conditions

$$\mathcal{P}^+ = 0 \quad \text{on } \partial D_D, \quad \frac{\partial \mathcal{P}^+}{\partial \nu} - ik\lambda\mathcal{P}^+ = 0 \quad \text{on } \partial D_I.$$

Since k is not an exterior eigenvalues we can conclude that $\mathcal{P} = 0$ outside D also. One more application of the above jump relations implies that $\phi = 0$ and $\psi = 0$, which proves the lemma. \square

3.1. Reconstruction of ∂D

Now we have all the ingredients to prove the main theorem related to the solvability of the data equation, which provides the theoretical basis of the linear sampling method. To this end, let us consider a particular case of the exterior mixed boundary condition (6), namely:

$$\begin{cases} \Delta u_z + k^2 u_z = 0 & \text{in } \mathbb{R}^2 \setminus \bar{D}, \\ u_z = -\Phi(\cdot, z) & \text{on } \partial D_D, \\ \frac{\partial u_z}{\partial \nu} - ik\lambda(x)u_z = -\frac{\partial \Phi(\cdot, z)}{\partial \nu} + ik\lambda(x)\Phi(\cdot, z) & \text{on } \partial D_I, \\ \lim_{r \rightarrow \infty} \sqrt{r} \left(\frac{\partial u_z}{\partial r} - ik u_z \right) = 0. \end{cases} \quad (13)$$

THEOREM 3.5 *Assume that k is not an exterior eigenvalue. Let u^s be the scattered field corresponding to the scattering problem (2) and M is the associated data operator given by (9). Then the following holds:*

- (1) For $z \in \mathbb{R}^2 \setminus \bar{D}$ and a given $\epsilon > 0$ there exists a function $g_z^\epsilon \in L^2(C)$ such that

$$\|Mg_z^\epsilon - \Phi(\cdot, z)\|_{L^2(C)} < \epsilon, \quad (14)$$

and as $\epsilon \rightarrow 0$, the potential $\omega_{g_z^\epsilon}$ given by (12) with kernel g_z^ϵ converges to the solution u_z of (13) in the $H^1(B_R \setminus \bar{D})$ -norm, for any large disk B_R containing D .

- (2) For $z \in D \setminus C$, every $g_z^\epsilon \in L^2(C)$ that satisfies (14) for a given $\epsilon > 0$ is such that

$$\lim_{\epsilon \rightarrow 0} \|\omega_{g_z^\epsilon}\|_{H^1(B_R \setminus \bar{D})} = \infty.$$

Proof For a given $\epsilon > 0$, from Lemma 3.2 there exists a function $f_z \in H^{\frac{1}{2}}(\partial D_D)$ and $h_z \in H^{-\frac{1}{2}}(\partial D_I)$ such that $B(f_z, h_z) = -\Phi(x, z)$ for $x \in C$. By means of Lemma 3.4, we can choose $g_z^\epsilon \in L^2(C)$ such that it satisfies

$$\|Hg_z^\epsilon - (f_z, h_z)\|_{H^{\frac{1}{2}}(\partial D_D) \times H^{-\frac{1}{2}}(\partial D_I)} < \frac{\epsilon}{\|B\|}.$$

Then (14) follows from the fact that $M = -BH$. Obviously $f_z = -\Phi(x, z)|_{\partial D_D}$ and $h_z = -\frac{\partial \Phi(\cdot, z)}{\partial \nu} + ik\lambda\Phi(\cdot, z)$. Now for $z \in \mathbb{R}^2 \setminus \bar{D}$ from the well-posedness of (13), the convergence of the boundary data $Hg_z^\epsilon - (f_z, h_z) \rightarrow 0$ as $\epsilon \rightarrow 0$ in the $H^{\frac{1}{2}}(\partial D_D) \times H^{-\frac{1}{2}}(\partial D_I)$ -norm implies convergence of the corresponding solutions $\omega_{g_z^\epsilon} \rightarrow u_z$ as $\epsilon \rightarrow 0$ in $H_{loc}^1(\mathbb{R}^2 \setminus \bar{D})$ of the exterior mixed boundary value problem. This proves the first statement. Note that for a fixed $\epsilon > 0$, we have that

$$\lim_{z \rightarrow \partial D} \|\omega_{g_z^\epsilon}\|_{H^1(B_R \setminus \bar{D})} = \infty, \quad \text{and} \quad \lim_{z \rightarrow \partial D} \|g_z^\epsilon\|_{L^2(C)} = \infty$$

where z approached ∂D from outside of D .

In order to prove the second statement, let $z \in D \setminus C$ and assume to the contrary that there exists a sequence $\{\epsilon_n\} \rightarrow 0$ and the corresponding function ω_n with kernels $g_n := g_z^{\epsilon_n}$ satisfying (14) is such that $\|\omega_n\|_{H_{loc}^1(\mathbb{R}^2 \setminus \bar{D})}$ remains bounded. From the trace theorem, $\|Hg_n\|_{H^{\frac{1}{2}}(\partial D_D) \times H^{-\frac{1}{2}}(\partial D_I)}$ is also bounded. Then without loss of generality we may assume

weak convergence $Hg_n \rightharpoonup (f, h)$ as $n \rightarrow \infty$ for some $(f, h) \in H^{\frac{1}{2}}(\partial D_D) \times H^{-\frac{1}{2}}(\partial D_I)$. Then, $BHg_n \rightharpoonup B(f, h)$ in $L^2(C)$. But $BHg_n \rightarrow -\Phi(\cdot, z)|_C$ which means $-\Phi(\cdot, z) = B(f, g)$. This contradicts Lemma 3.3. \square

This theorem can be used to reconstruct the boundary ∂D , since roughly it says that, for fixed ϵ , if g_z^ϵ is the approximate solution of $Mg_z^\epsilon = \Phi(\cdot, z)$ than $\|\omega_{g_z^\epsilon}\|_{H^1(B_R \setminus \bar{D})}$ is large for z in D and small for z outside D . Unfortunately, $\|\omega_{g_z^\epsilon}\|_{H^1(B_R \setminus \bar{D})}$ can not be used as indicator function for D since it depends on D . Instead in practice we construct the indicator function $I(z) := \|g_z^\epsilon\|_{L^2(C)}$. It is not possible to prove a similar type of statement of $I(z)$ and in the above theorem, although all numerical examples confirm that $I(z)$ inherit the same behaviour as $\|\omega_{g_z^\epsilon}\|_{H^1(B_R \setminus \bar{D})}$. This short come of the linear sampling method for simple exterior inverse scattering problems is removed using the factorization method.[22,23] Unfortunately, for our scattering problem the factorization method is not valid and thus a mathematical proof for the behavior of $I(z)$ remains an open problem.

The linear sampling method for reconstruction of ∂D can now be described as follows.

- (1) Choose a set of sampling points in a region covering the expected obstacle.
- (2) For each sampling point z , solve the data equation (10) using Tikhonov regularization technique, i.e. solve

$$\alpha g + M^* M g = M^* \Phi(\cdot, z) \tag{15}$$

with regularization parameter $\alpha > 0$ (note that M is compact operator, therefore the data equation is ill-posed).

- (3) Calculate the indicator function $I(z)$.
- (4) Plot $I(z)$ and the obstacle D is the region containing points z for which $I(z) > C$ for a cut-off value C chosen by ad-hoc procedure (some procedures for choosing C are available in the literature, see e.g. [2,24,25]).

3.2. Determination of the surface impedance

Having determined the shape of the cavity D , we now turn our attention to determining the boundary impedance $\lambda \in L_\infty(\partial D_I)$. First we give a uniqueness proof for $\lambda \in L_\infty(\partial D_I)$ (note that λ bounded function is not covered by Theorem 2.1) using multistatic data i.e. many point sources and measurements. This proof is more in the spirit of our reconstruction technique. To this end, let ω_g^s be the scattered field due to the incident field ω_g given by (12), i.e. the solution of (13) with $\Phi(\cdot, z)$ replaced by ω_g . Note that the data Mg defined by (10) equals to ω_g^s evaluated on C .

LEMMA 3.6 *Let $\omega_g^t := \omega_g^s + \omega_g$. Then*

$$\int_{\partial D_D} \lambda(x) |\omega_g^t|^2 ds = \int_S |\omega_{g,\infty}|^2 ds + \frac{1}{k} \text{Im}(Mg, g), \tag{16}$$

where S is the unit circle, $\omega_{g,\infty}$ is the far-field pattern of the radiating field ω_g [5] and (\cdot, \cdot) denotes the $L^2(C)$ -inner product.

Proof The proof follows the ideas in [26]. Applying the boundary conditions $\omega_g^t = 0$ on ∂D_D and $\frac{\partial \omega_g^t}{\partial \nu} - ik\lambda \omega_g^t = 0$ on ∂D_I together with Green's identity, we obtain that

$$\begin{aligned} -2ik \int_{\partial D_D} \lambda(x) |\omega_g^t|^2 ds &= \int_{\partial D} \left[\omega_g^t \frac{\partial \overline{\omega_g^t}}{\partial \nu} - \overline{\omega_g^t} \frac{\partial \omega_g^t}{\partial \nu} \right] ds \\ &= \int_{\partial D} \left[\omega_g^s \frac{\partial \overline{\omega_g^s}}{\partial \nu} - \overline{\omega_g^s} \frac{\partial \omega_g^s}{\partial \nu} \right] ds + \int_{\partial D} \left[\omega_g \frac{\partial \overline{\omega_g}}{\partial \nu} - \overline{\omega_g} \frac{\partial \omega_g}{\partial \nu} \right] ds \\ &\quad + \int_{\partial D} \left[\omega_g^s \frac{\partial \overline{\omega_g}}{\partial \nu} - \overline{\omega_g} \frac{\partial \omega_g^s}{\partial \nu} \right] ds + \int_{\partial D} \left[\omega_g \frac{\partial \overline{\omega_g^s}}{\partial \nu} - \overline{\omega_g^s} \frac{\partial \omega_g}{\partial \nu} \right] ds. \end{aligned} \quad (17)$$

First note that the first term in (17) is zero. From Green's theorem applied to the radiating solution ω_g of the Helmholtz equation in $\mathbb{R}^2 \setminus \overline{D}$, we have that

$$\int_{\partial D} \left[\omega_g \frac{\partial \overline{\omega_g}}{\partial \nu} - \overline{\omega_g} \frac{\partial \omega_g}{\partial \nu} \right] ds = -2ik \int_S |\omega_{g,\infty}|^2 ds. \quad (18)$$

Furthermore, since $\omega_g(x) = \int_C \Phi(x, y) g(y) ds(y)$, by changing the order of integration we obtain that

$$\begin{aligned} &\int_{\partial D} \left[\omega_g^s \frac{\partial \overline{\omega_g}}{\partial \nu} - \overline{\omega_g} \frac{\partial \omega_g^s}{\partial \nu} \right] ds(x) \\ &= \int_C \overline{g(y)} \int_{\partial D} \left(\omega_g^s(x) \frac{\partial \overline{\Phi(x, y)}}{\partial \nu} - \overline{\Phi(x, y)} \frac{\partial \omega_g^s(x)}{\partial \nu} \right) ds(x) ds(y) \\ &= - \int_C \overline{g(y)} \omega_g^s(y) ds(y). \end{aligned} \quad (19)$$

Plugging (18) and (19) into (17), we finally obtain

$$\begin{aligned} -2ik \int_{\partial D} \lambda(x) |\omega_g^t|^2 ds(x) &= -2ik \int_S |\omega_{g,\infty}|^2 ds - \int_C \overline{g(y)} \omega_g^s(y) ds(y) \\ &\quad + \int_C g(y) \overline{\omega_g^s(y)} ds(y) \\ &= -2ik \int_S |\omega_{g,\infty}|^2 ds + (g, Mg) - (Mg, g) \\ &= -2ik \int_S |\omega_{g,\infty}|^2 ds - 2i \operatorname{Im}(Mg, g). \end{aligned}$$

Dividing both sides by $-2ik$ yields the result. \square

THEOREM 3.7 *The impedance function $\lambda \in L_\infty(\partial D_I)$, is uniquely determined from a knowledge of the data operator M defined by (10).*

Proof The proof is base on the identity (16). Since the left-hand side of (16) is known from the data for all g , we need to show that the set \mathcal{W}

$$\mathcal{W} := \left\{ f \in L^2(\partial D_I) : \begin{array}{l} f = \omega_g^t|_{\partial D_I} \text{ for some } g \in L^2(C) \\ \text{where } \omega_g^t \text{ is as in Lemma 3.6.} \end{array} \right\}$$

is dense in $L^2(\partial D_I)$. To this end assume that ϕ is a function in $L^2(\partial D_I)$ such that for all $f = \omega_g^t|_{\partial D_I} \in W$

$$\int_{\partial D_I} \omega_g^t \phi ds = 0.$$

Construct $u \in H^1(D)$ as the unique solution of the interior mixed boundary value problem

$$\begin{cases} \Delta u + k^2 u = 0 & x \in D, \\ u = 0 & x \in \partial D_D, \\ \frac{\partial u}{\partial \nu} - ik\lambda u = \phi & x \in \partial D_I. \end{cases}$$

Then using that $(\omega_g^s + \omega_g) = 0$ on ∂D_D and $ik\lambda(\omega_g^s + \omega_g) = \frac{\partial}{\partial \nu}(\omega_g^s + \omega_g)$ on ∂D_I we have that

$$\begin{aligned} 0 &= \int_{\partial D} (\omega_g^s + \omega_g) \left(\frac{\partial u}{\partial \nu} - ik\lambda u \right) ds \\ &= \int_{\partial D} \left(\omega_g^s \frac{\partial u}{\partial \nu} - u \frac{\partial \omega_g^s}{\partial \nu} \right) ds + \int_{\partial D} \left(\omega_g \frac{\partial u}{\partial \nu} - u \frac{\partial \omega_g}{\partial \nu} \right) ds \\ &= \int_{\partial D} \left(\omega_g \frac{\partial u}{\partial \nu} - u \frac{\partial \omega_g}{\partial \nu} \right) ds \end{aligned}$$

for all $g \in L^2(C)$. From the definition of ω_g and Green's representation theorem by changing the order of integration, we can conclude that

$$0 = \int_{\partial D} \left(\Phi(x, y) \frac{\partial u}{\partial \nu}(x) - u(x) \frac{\partial \Phi(x, y)}{\partial \nu} \right) ds = u(y)$$

which yields $\phi = 0$ from the trace theorem.

Now assume that λ_1 and λ_2 yield to the same data operator M . Then from Lemma 3.6 we have that

$$\int_{\partial D_I} [\lambda_1(x) - \lambda_2(x)] |\omega_g^t|^2 dx = 0.$$

Viewing the $L_\infty(\partial D_I)$ function $\lambda_1 - \lambda_2$ as a self-adjoint operator on $L^2(\partial D_I)$, since \mathcal{W} is dense in $L^2(\partial D_I)$ we conclude that $\lambda_1(x) = \lambda_2(x)$ almost everywhere on ∂D_I (see e.g. Theorem 9.2-2 of [27]). Note that we have already proven in Theorem 2.1 uniqueness for ∂D_I . \square

The rest of the paper is devoting to deriving reconstruction formulas for λ . Let us recall $u_z \in H_{loc}^1(\mathbb{R}^2 \setminus \bar{D})$ which is the solution of the exterior mixed boundary value problem (13), provided that k is not an exterior eigenvalue and define

$$v_z := u_z + \Phi(\cdot, z). \tag{20}$$

The following lemma will provide the key ingredient for determining λ from a knowledge of the data operator M .

LEMMA 3.8 *Assume that k is not an exterior eigenvalue. For every $z_1, z_2 \in \mathbb{R}^2 \setminus \bar{D}$ we have that*

$$\int_{\partial D_I} v_{z_1} \lambda \bar{v}_{z_2} ds = \int_S u_{z_1, \infty} \overline{u_{z_2, \infty}} ds - \frac{i}{2k} (\bar{u}_{z_2}(z_1) - u_{z_1}(z_2)), \tag{21}$$

where S is the unit circle.

Proof By applying Green's second identity, the zero mixed boundary conditions for v_z and Lemma 2.1 in [26] we have that

$$\begin{aligned}
 -2ik \int_{\partial D_I} v_{z_1} \lambda(x) \bar{v}_{z_2} ds &= \int_{\partial D} \left[v_{z_1} \frac{\partial \bar{v}_{z_2}}{\partial \nu(x)} - \bar{v}_{z_2} \frac{\partial v_{z_1}}{\partial \nu(x)} \right] ds \\
 &= \int_{\partial D} \left[\Phi(\cdot, z_1) \frac{\partial \overline{\Phi(\cdot, z_2)}}{\partial \nu} - \overline{\Phi(\cdot, z_2)} \frac{\partial \Phi(\cdot, z_1)}{\partial \nu} \right] ds \\
 &\quad + \int_{\partial D} \left[u_{z_1} \frac{\partial \overline{\Phi(\cdot, z_2)}}{\partial \nu} - \overline{\Phi(\cdot, z_2)} \frac{\partial u_{z_1}}{\partial \nu} \right] ds \\
 &\quad + \int_{\partial D} \left[\Phi(\cdot, z_1) \frac{\partial \bar{u}_{z_2}}{\partial \nu} - \bar{u}_{z_2} \frac{\partial \Phi(\cdot, z_1)}{\partial \nu} \right] ds \\
 &\quad + \int_{\partial D} \left[u_{z_1} \frac{\partial \bar{u}_{z_2}}{\partial \nu} - \bar{u}_{z_2} \frac{\partial u_{z_1}}{\partial \nu} \right] ds \\
 &= -(\bar{u}_{z_2}(z_1) + u_{z_1}(z_2)) - 2ik \int_S u_{z_1, \infty} \overline{u_{z_2, \infty}} ds.
 \end{aligned}$$

Finally, dividing both sides by $2ik$ yields the identity. □

In particular, setting $z := z_1 = z_2$ the identity in Lemma 3.8 can be re-written as in the following lemma.

LEMMA 3.9 *Assume that k is not an exterior eigenvalue. For every $z \in \mathbb{R}^2 \setminus \bar{D}$ the following holds*

$$\int_{\partial D_I} \lambda(x) |u_z + \Phi(\cdot, z)| ds = \int_S |u_{z, \infty}|^2 ds - \frac{1}{k} \text{Im } u_z(z). \tag{22}$$

LEMMA 3.10 *Let $\mathcal{B} \subset \mathbb{R}^2 \setminus \bar{D}$ be a open region and define*

$$\mathcal{V} := \left\{ f \in L^2(\partial D_I) : \begin{array}{l} f = u_z + \Phi(\cdot, z)|_{\partial D_I} \\ z \in \mathcal{B}, \text{ and } u_z \text{ the solution of (13)} \end{array} \right\}.$$

Then \mathcal{V} is complete in $L^2(\partial D_I)$.

Proof Assume that ϕ is a function in $L^2(\partial D_I)$ such that for every $z \in \mathcal{B}$

$$\int_{\partial D_I} (u_z + \Phi(\cdot, z))\phi ds = 0.$$

Construct $u \in H^1_{loc}(R^2 \setminus \bar{D})$ as the unique solution of the exterior mixed boundary value problem

$$\begin{cases} \Delta u + k^2 u = 0 & x \in D, \\ u = 0 & x \in \partial D_D, \\ \frac{\partial u}{\partial \nu} - ik\lambda u = \phi & x \in \partial D_I, \\ \lim_{r \rightarrow \infty} \sqrt{r} \left(\frac{\partial u}{\partial r} - iku \right) = 0 \end{cases}$$

which exists since k is not an exterior eigenvalue. Then for every $z \in \mathcal{B}$, using the zero mixed boundary conditions for $u_z + \Phi(\cdot, z)$, the integral representation formula and Green's second identity we have

$$\begin{aligned} 0 &= \int_{\partial D} (u_z + \Phi(\cdot, z)) \left(\frac{\partial u}{\partial \nu} - ik\lambda u \right) ds \\ &= \int_{\partial D} \left(u_z \frac{\partial u}{\partial \nu} - u \frac{\partial u_z}{\partial \nu} \right) ds + \int_{\partial D} \left(\Phi(\cdot, z) \frac{\partial u}{\partial \nu} - u \frac{\partial \Phi(\cdot, z)}{\partial \nu} \right) ds \\ &= -u(z), \quad \text{for } z \in \mathcal{B}. \end{aligned}$$

The unique continuation principle for solutions of the Helmholtz equation implies that $u = 0$ in all of $\mathbb{R}^2 \setminus \overline{D}$ which yields $\phi = 0$ from the trace theorem. \square

Remark 3.1 The result of Lemma 3.10 holds true if \mathcal{B} is a closed curve surrounding D . In this case, one uses the uniqueness of the exterior Dirichlet problem to conclude that $u = 0$ in the proof. We use this configuration of \mathcal{B} in our numerical example.

The equation (22) can be seen as an integral equation of the first kind for λ . Since $u_z + \Phi(\cdot, z)$ vanishes on ∂D_D we can replace the region of integration ∂D_I by ∂D . Using Lemma 3.10, it is easy to prove in the same way as in the proof of Theorem 3.7 that the left-hand side of this equation is an injective compact integral operator with $L_\infty(\partial D)$ positive kernel. What is more important, both the right-hand side of (22) and its kernel can be approximately computed using the measured data. In particular from the first part of Theorem 3.5, if g_z is the approximate solution of the data equation

$$(Mg_z)(x) = \Phi(x, z), \quad z \in \mathbb{R}^2 \setminus \overline{D},$$

then

$$\omega_{g_z}(x) = \int_C \Phi(x, y) g_z(y) ds(y)$$

approximates u_z . Note that this g_z is the same function used in the linear sampling method to construct the indicator function $I(z)$ of D .

In practice, having determined D based on the Tikhonov regularized solution to

$$\alpha g + M^* M g = M^* \Phi(\cdot, z)$$

for z in an open region $\mathcal{B} \subset \mathbb{R}^2 \setminus \overline{D}$ we compute ω_{g_z} and then solve the integral equation for λ

$$\int_{\partial D} \lambda(x) |\omega_{g_z} + \Phi(\cdot, z)| ds = \int_S |\omega_{g_{z,\infty}}|^2 ds - \frac{1}{k} \text{Im } \omega_{g_{z,\infty}}(z)$$

where $\omega_{g_{z,\infty}}(\hat{x}) = \gamma \int_C e^{-ik\hat{x}\cdot y} g_{z,\infty}(y) ds(y)$, $\gamma = \frac{e^{i\pi/4}}{\sqrt{8\pi k}}$.

In the particular case when the surface impedance is a positive constant $\lambda > 0$, we obtain a simpler formula for λ , namely

$$\lambda \approx \frac{\int_S |\omega_{g_{z,\infty}}(\hat{x})|^2 ds(\hat{x}) - \frac{1}{k} \text{Im } (\omega_{g_z}(z))}{\|\omega_{g_z}(\cdot) + \Phi(\cdot, z)\|_{L^2(\partial D)}^2}, \quad z \in \mathbb{R}^2 \setminus \overline{D} \tag{23}$$

Note that we do not need to know a priori which part of the boundary is coated in order to reconstruct λ .

4. Numerical examples

We now illustrate the theoretical results of the previous sections with some numerical examples. We simulate the data for our numerical examples by solving the corresponding mixed boundary value problem for chosen D , ∂D_D and λ to obtain $u^\delta(x, y)$, $x, y \in C$ (to simulate the mixed boundary value problem, in fact we solve an impedance boundary value problem with chosen λ on ∂D_I and with $\lambda = 10^{10}$ on ∂D_D which is a good approximation to Dirichlet boundary condition; $\lambda \rightarrow +\infty$ corresponds to Dirichlet boundary condition). This impedance problem is solved using an integral equation approach [12] which is discretized based on the Nyström's method [21]. For numerical solution of the data integral equation (10), we use the trapezoidal rule to obtain an ill-conditioned matrix system $M^\delta g_z = b_z$, in which z is chosen between two rectangular grids B_1 and B_2 , such that $C \subset B_2 \subset D \subset B_1$. Here M^δ is the discrete version of Mg corrupted by random noise in the following way: each element $(m_{i,j}^\delta)$ of the matrix M^δ is given by $M_{i,j}^\delta = M_{i,j}(1 + \delta \Delta_{i,j})$, where δ denotes the error level and $\Delta_{i,j} \in (-1, 1)$ is obtained by a random number generator. Since (10) is severely ill-posed, [21, 28, 29] we use the Tikhonov regularization method [29] to solve (15) where the regularization parameter α is chosen by using the generalized cross-validation criterion. [30, 31] Note that α depends on the sampling point z .

In our examples, we consider two different geometries for the cavity, namely the kite and the peanut.

Example 1 The kite. We consider the cavity D with boundary

$$\partial D = \{x : x = (x_1, x_2) = (2.2 \cos(t) + 1.25 \cos(2t) - 1.25, 3 \sin t), t \in [0, 2\pi]\}.$$

Example 2 The peanut. We consider the cavity D with boundary

$$\partial D = \{x : x = (x_1, x_2) = (2 \cos(t) + 0.4 \cos(3t), 2 \sin(t) + 0.4 \sin(3t)), t \in [0, 2\pi]\}.$$

It has been shown in Theorem 3.5 that, for $z \in \mathbb{R}^2 \setminus \bar{D}$, $\omega_g \approx u_z$, where ω_g and u_z are defined by (12) and (13), respectively, and our numerical examples confirm this fact. In particular, we choose a point $z = (5, 0)$ outside the scatterer D and plot the values of ω_g on a circle with radius 5 which are shown in Figure 1 together with the corresponding values of u_z . Consider the ill-posed nature of the problem, ω_g gives a very good approximation of u_z as expected.

4.1. Reconstruction of the obstacle shape ∂D

In the following numerical computations, we always choose the curve C to be a circle whose radius is $r_c = 0.15$ centred at the origin and set 1.6 the side length of the small square B_2 between ∂D and the curve C . We also choose 64 source points and measurements points distributed equidistantly on the curve C and compute the corresponding g_z . To visualize the obstacle we plot the level curves of the logarithmic of the discrete l_2 norm of g . For both shapes, we specify the Dirichet boundary condition for $t \in [0, \pi]$ and the impedance boundary condition with $\lambda = 8$ for $t \in [\pi, 2\pi]$. The numerical results of the reconstructions of the kite and the peanut with $k = 1$ are shown in Figures 2 and 3, respectively.

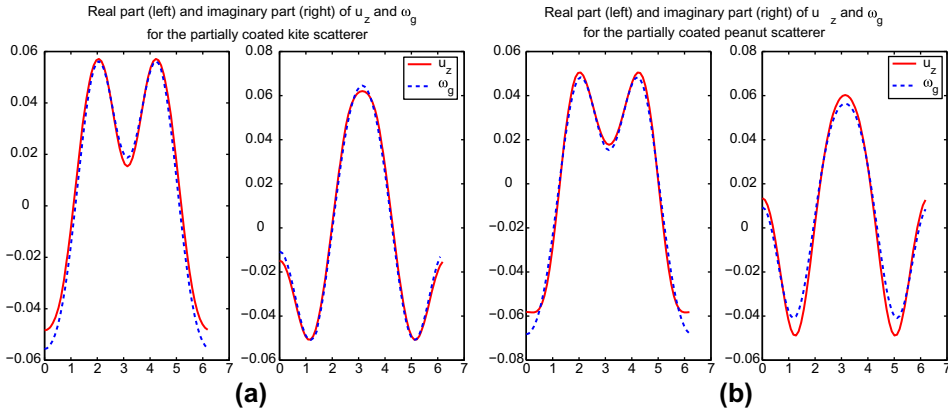


Figure 1. The real part and imaginary part of u_z and ω_g for $z = (5, 0)$ corresponding to $k = 1$, D is the kite (a) and the peanut (b) respectively with impedance boundary condition for $t \in [\pi, 2\pi]$ with $\lambda = 8$.

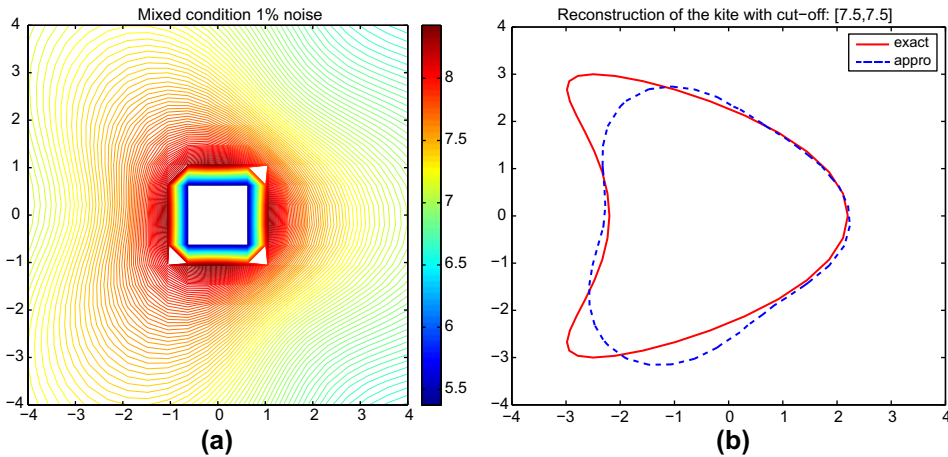


Figure 2. Reconstruction of a kite with mixed boundary condition with 1% noise. Dirichet boundary condition is given for $t \in [0, \pi]$ and the impedance boundary condition with $\lambda = 8$ for $t \in [\pi, 2\pi]$. The dotted curve that approximates the boundary in the Figure on the right is one of the level curves. To view a colour version of this figure please see the online version of the article.

4.2. Reconstruction of the surface impedance λ

Having obtained the boundary of the cavity using the linear sampling method, we now want to determine the surface impedance λ .

We first consider the case of a totally coated i.e. with impedance boundary condition on the whole of ∂D and $\partial D_D = \emptyset$, assuming that the boundary is known exactly scatterer. Again, the measurement curve C is the circle of radius 0.15 centred at the origin. In our first example, we consider constant impedance $\lambda = 1$. We choose a circle \mathcal{B}_r centred at the origin of radius 5, and use 64 sampling points z on \mathcal{B}_r . For each z we calculate the surface impedance λ according to (23). The computed values of $\lambda = 1$ for different wave numbers

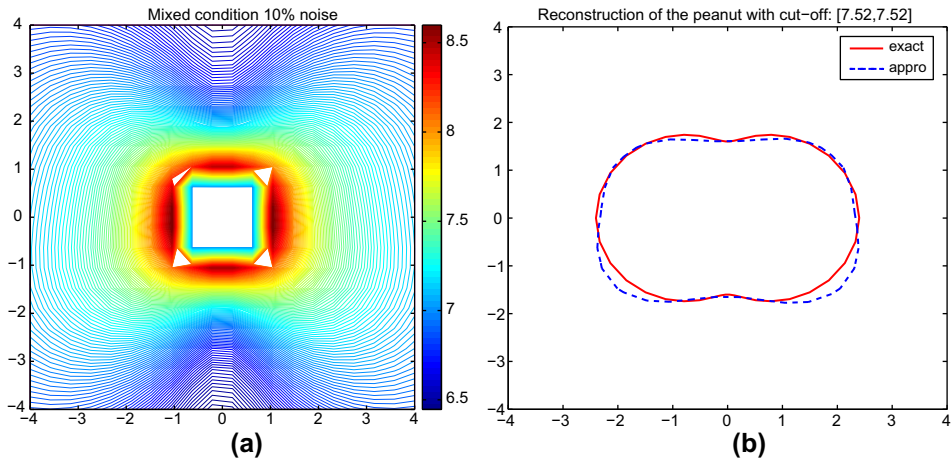


Figure 3. Reconstruction of a peanut with mixed boundary condition with 10% noise. Dirichlet boundary condition is given for $t \in [0, \pi]$ and the impedance boundary condition with $\lambda = 8$ for $t \in [\pi, 2\pi]$. The dotted curve that approximates the boundary in the Figure on the right is one of the level curves. To view a colour version of this figure please see the online version of the article.

Table 1. The reconstruction of the surface impedance $\lambda = 1$ for the kite scatterer using different wave numbers.

Wave number	Maximum	Average	Median
$k = 1$	1.0676	0.9205	0.9026
$k = 2$	1.0217	0.9126	0.9040
$k = 4$	1.0005	0.8702	0.8901

Table 2. The reconstruction of the surface impedance $\lambda = 1$ for the peanut scatterer using different wave numbers.

Wave number	Maximum	Average	Median
$k = 1$	1.0455	0.9168	0.9081
$k = 2$	1.0535	1.0390	1.0421
$k = 4$	1.0394	0.9565	0.9403

give a very good approximation to the surface impedance as shown in Table 1 for the kite and Table 2 for the peanut.

In the next examples, we reconstruct a piecewise constant and a function impedance by solving (22) using the Tikhonov regularization with regularization parameter α chosen by trial and error. We fix $k = 1$, take D to be the kite defined in Example 2 and $z \in \mathcal{B}_r$ as described above. The reconstructions for $\lambda(x)$ given by

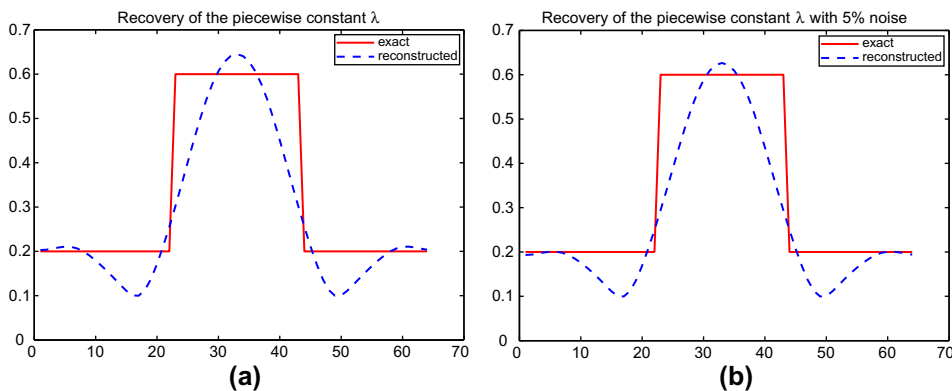


Figure 4. Reconstruction of piecewise constant λ with exact data on the left and with 5% noisy data on the right.

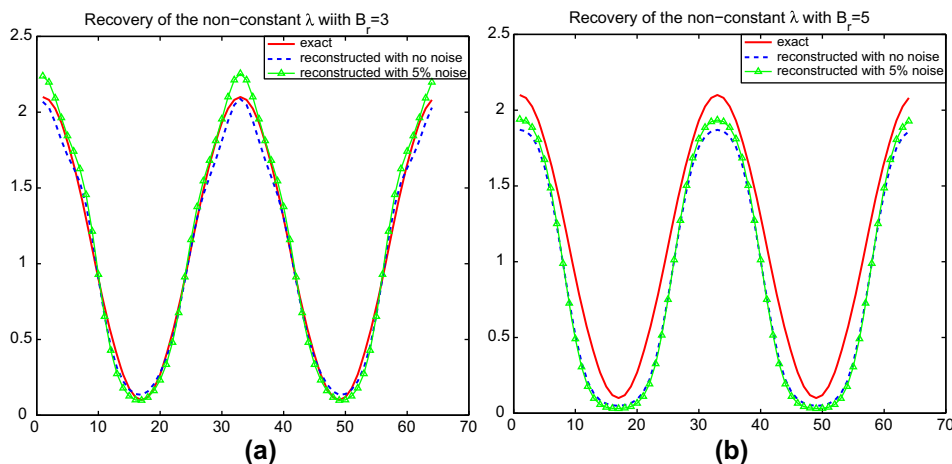


Figure 5. Reconstruction of non-constant λ : on the left for \mathcal{B}_3 and on the right for \mathcal{B}_5 . To view a colour version of this figure please see the online version of the article.

$$\lambda(x(t)) = \begin{cases} 0.2 & 0 \leq t < \frac{2}{3}\pi, \\ 0.6 & \frac{2}{3}\pi \leq t < \frac{4}{3}\pi, \\ 0.2 & \frac{4}{3}\pi \leq t \leq 2\pi. \end{cases} \quad (24)$$

is presented in Figure 4. The exact near-field data are used in Figure 4(a). To test the stability of our inversion method, we use the noisy near-field data with $\delta = 5\%$ in Figure 4(b).

Finally, we consider a function impedance given by

$$\lambda(x(t)) = 1.1 + \cos(2t), \quad t \in [0, 2\pi] \quad (25)$$

on the boundary of the kite. Using the exact near-field data and the noisy data with $\delta = 5\%$, the reconstruction of the impedance function λ given by (25) with point z situated on different circles \mathcal{B}_r containing D are exhibited in Figure 5.

The above numerical examples indicate that our proposed reconstruction method provides good stable reconstructions of both the shape of cavity and the surface impedance function in an efficient way. The drawback is that it requires a lot of measurements. More analysis is needed to understand the integral equation (22) and also more numerical tests are needed for the case of mixed boundary conditions with function impedance λ .

Acknowledgements

The research of Y.Q.Hu and J.J.Liu are supported by NSFC No.11161130002, No.11071039 and the Fundamental Research Funds for the Central Universities No. 3207011102. The research of F. Cakoni is supported in part by the Air Force Office of Scientific Research Grant FA9550-11-1-0189 and NSF Grant DMS-1106972.

References

- [1] Cakoni F, Colton D. *Qualitative methods in inverse scattering theory*. Berlin: Springer; 2006.
- [2] Cakoni F, Colton D, Monk P. *The linear sampling method in inverse electromagnetic scattering*, CBMS Series, Vol. 80. SIAM Publications; 2011.
- [3] Kirsch A, Grinberg N. *The factorization method for inverse problems*. New York: Oxford University Press; 2008.
- [4] Potthast R. A point source method for inverse acoustic and electromagnetic obstacle scattering problems. *IMA Journal of Applied Mathematics*. 1998;61(2):119–140.
- [5] Colton D, Kress R. *Inverse acoustic and electromagnetic scattering theory*. 3rd ed. New York: Springer; 2013.
- [6] Cakoni F, Colton D, Monk P. The direct and inverse scattering problems for partially coated obstacles. *Inverse Problems*. 2001;17:1997–2015.
- [7] Cakoni F, Colton D. The determination of the surface impedance of a partially coated obstacle from far field data. *SIAM Journal on Applied Mathematics*. 2004;64:709–723.
- [8] Cakoni F, Colton D, Monk P. The determination of the surface conductivity of a partially coated dielectric. *SIAM Journal on Applied Mathematics*. 2005;65:767–789.
- [9] Cakoni F, Kress R, Schuft C. Integral equations for shape and impedance reconstruction in corrosion detection. *Inverse Problems*. 2010; 26(9) [paper 095012].
- [10] Liu JJ, Nakamura G, Sini M. Reconstruction of the shape and surface impedance for acoustic scattering data for an arbitrary cylinder. *SIAM Journal on Applied Mathematics*. 2007;67(4):1124–1146.
- [11] Wang HB, Liu JJ. On the reconstruction of surface impedance from the far-field data in inverse scattering problems. *Applicable Analysis*. 2012;91(4):787–806.
- [12] Qin HH, Colton D. The inverse scattering problem for cavities with impedance boundary condition. *Journal of Advances in Computational Mathematics*. 2012;36(2):157–174.
- [13] Qin HH, Colton D. The inverse scattering problem for cavities. *Journal of Applied Numerical Mathematics*. 2012;62:699–708.
- [14] Zeng F, Cakoni F, Sun J. An inverse electromagnetic scattering problem for cavity. *Inverse Problems*. 2011;27(12):125002.
- [15] Qin HH, Cakoni F. Nonlinear integral equations for shape reconstruction in the inverse interior scattering problem. *Inverse Problems*. 2011;27(3):035005.
- [16] Ikehata M, Itou H. On reconstruction of a cavity in a linearized viscoelastic body from infinitely many transient boundary data. *Inverse Problems*. 2012;28:125003.
- [17] Ikehata M, Itou H. An inverse acoustic scattering problem inside a cavity with dynamical back-scattering data. *Inverse Problems*. 2012;28:095016.
- [18] Jakubik P. Testing the integrity of some cavity-the Cauchy problem and the range test. *Applied Numerical Mathematics*. 2008;58:899–914.

- [19] Nakamura G, Sini M. Obstacle and boundary determination from scattering data. *SIAM Journal on Mathematical Analysis*. 2007;39:819–837.
- [20] McLean W. *Strongly elliptic systems and boundary integral equations*. Cambridge: Cambridge University Press; 2000.
- [21] Kress R. *Linear integral equations*. Berlin: Springer-Verlag; 1989.
- [22] Arens T. Why linear sampling works. *Inverse Problems*. 2004;20(1):163–173.
- [23] Arens T, Lechleiter A. The linear sampling method revisited. *Journal of Integral Equations and Applications*. 2009;21(2):179–202.
- [24] Collino F, Fares MB, Haddar H. Numerical and analytical studies of the linear sampling method in electromagnetic inverse scattering problems. *Inverse Problems*. 2003;19(6):1279–1298.
- [25] Li JZh. Strengthened linear sampling method with a reference ball. *SIAM Journal on Applied Mathematics*. 2009;31(6):4013–4040.
- [26] Colton D, Kress R. Eigenvalues of the far field operator and inverse scattering theory. *SIAM Journal on Mathematical Analysis*. 1995;26:601–615.
- [27] Kreyszig E. *Introductory functional analysis with applications*. New York: John Wiley; 1978.
- [28] Hadamard J. *Lectures on Cauchy's Problem in Linear Partial Differential Equations*. New York: Dover Publications; 1953.
- [29] Kirsch A. *An introduction to the mathematical theory of inverse problems*. Berlin: Springer; 1996.
- [30] Hansen PC. Analysis of discrete ill-posed problems by means of the L-curve. *SIAM Review*. 1992;34:561–580.
- [31] Hansen PC. Regularization tools: a Matlab package for analysis and solution of discrete ill-posed problems. *Numerical Algorithms*. 1994;6:1–35.
- [32] Cakoni F, Monk P. The determination of anisotropic surface impedance in electromagnetic scattering. *Journal on Methods and Applications of Analysis*. 2010;17(4):379–394.
- [33] Liu JJ, Sini M. On the accuracy of the numerical detection of complex obstacles from far field data using the probe method. *SIAM J. Sci. Comput.* 2009;31(4):2665–2687.